ISSN 2176-5480

22nd International Congress of Mechanical Engineering (COBEM 2013)
November 3-7, 2013, Ribeirão Preto, SP, Brazil

STIFFNESS VARIATION OF E-GLASS/EPOXY ADAPTATIVE BEAMS INCORPORATING Ni-Ti EMBEDDED WIRES

Peter Faluhelyi
Flaminio Levy-Neto
Universidade de Brasília, UnB-FT-ENM, Dept. Eng. Mecânica, Asa Norte, 70910-900, Brasilia – DF - Brazil
pyi@brturbo.com.br, flaminio@unb.br

Abstract. *This study evaluates the variation of the flexural modulus of adaptavive beams, subjected to three point bending. The beams have nineteen layers of epoxy reinforced with chopped E-glass mat (17 plies), and two symmetric active plies (A) embedded with up to four Ni-Ti wires each (2+A+13+A+2). The beams were manufactured using a closed metallic mould, with a device to stretch the wires. At 25 ^{0}C, the Ni-Ti wires are in martensitic phase and present elasticity modulus of 22.6 GPa. When the temperature of the wires is raised to 69 ^{0}C, an austenitic transformation occurs and the elasticity modulus increases to 48.4 GPa. One of the purposes of this investigation is to verify how the bending modulus of the beams changes, when electric current passes through the wires and elevates their temperature to 69 ^{0}C. In addition, using the finite element program ANSYS, carryout a modal analysis to obtain the effects of the temperature variation on the natural frequencies of the beams. The bending tests followed ASTM standard D-790-08 and the theoretical effective flexural modulus (E_f), based on macromechanics, was compared with the experimental results. The experimental results showed that the bending modulus of the tested beams increased up to 9.07%, incorporating a volume fraction of 1.74% of Ni-Ti wires and changing their temperatures from 25 ^{0}C to 69 ^{0}C. Theoretically the increasing in E_f was 9.25%.*

Keywords: *adaptative composite beams, bending stiffness*

1. INTRODUCTION

Polymeric composites combine at least two distinct phases, and are well known by their high specific strength and stiffness, which allow the creation of light structural components (Daniel and Ishai, 2006; Levy-Neto and Pardini, 2006). The continuous phase, the matrix, agglutinates and protects the reinforcement. The composites investigated in the present study, designated by Rogers and Robertshaw (1989) as Shape Memory Alloy Hybrid Composites (SMAHC), are prismatic beams that incorporate a third constituent, Ni-Ti active wires. The development of Ni-Ti shape memory alloys (SMA) has paved the way for special applications in robotics, bioengineering and complex aerospace systems (Ghandi and Thomson, 1992; Janocha, 1999; Srinivasan and McFarland, 2001). With the addition of the Ni-Ti wires which, besides other features, increase their elasticity modulus when heated, SMAHC can be regarded as adaptative or smart structures. The development of smart/intelligent composite structures, incorporating SMA, has become an attractive research topic in engineering, due to their capacity to work as a sensor or actuator (Turner, 2000).

Adaptative composite structures with embedded active Ni-Ti wires, are able to respond to external inputs, for example a moderate increase in temperature (e.g. from 25 °C to 69 °C). These SMA wires change their elasticity modulus, by a factor of almost three times, as showed in Figure 1, when a controlled electric current warms up the wires (Srinivasan & McFarland, 2001). Thus, a SMAHC component can present different mechanical behavior and adapt itself to service and environmental conditions. The controlled variation of the elasticity modulus, presented by SMA, for instance the Ni-Ti alloys, have motivated the application of such special alloys in many situations, for structural as well as machine vibration control and the optimization of different mechanical systems (Otsuka and Wayman, 1998).

The special properties presented by the Ni-Ti alloys depends on the transformation of the crystal structure, from the relatively softer martensitic phase, at lower temperatures (e.g. T < 25 ºC), to the stiffer austenite phase at higher temperatures (e.g. T > 69 ºC). During the initial development of Ni-Ti alloys, it was found that a composition consisting of nearly equal numbers of nickel and titanium atoms showed the transformation that leads to shape memory and an increase on the elasticity modulus (E). Further, by adding a slight extra amount of nickel in the alloy, it was possible to change the transformation temperature from near 100 ºC down to below 0 ºC. Also, this alloy had constituents that were not prohibitively expensive, and could be produced with existing metalworking techniques. The important temperatures at which phase transformations take place are known as: Ms ; Mf ; As ; as well as Af , and represent the temperatures of start (s) and finish (f) of martensitic (M) and austenitic (A) transformations, respectively (Srinivasan and McFarland, 2001). The main effect that is explored at the present work is the significant variation in stiffness (E) of the Ni-Ti wires, from E_M , at T < Ms in the martensitic phase, up to $E_A = 3.E_M$ (i.e. up to three times larger), at T > Af in the austenitic phase (Turner, 2000), as presented in Fig. 1. Thus, since the natural frequency of a component depends on its mass and stiffness, this frequency, in a SMAHC with embedded Ni-Ti wires, can be changed controlling the temperature of the wires. Meanwhile, the fabrication of SMAHC is complex and involves three different constituents in the same component. The main objectives of this work are: (i) the development of a fabrication method to produce 16

ISSN 2176-5480

SMAHC beams; and (ii) evaluate, the elastic properties and natural frequencies, of SMAHC beams with up to 8 embedded Ni-Ti wires, subjected to static and dynamical loads, at 25 °C (i.e. T < Mf) and to 69 °C (i.e. T > Af).

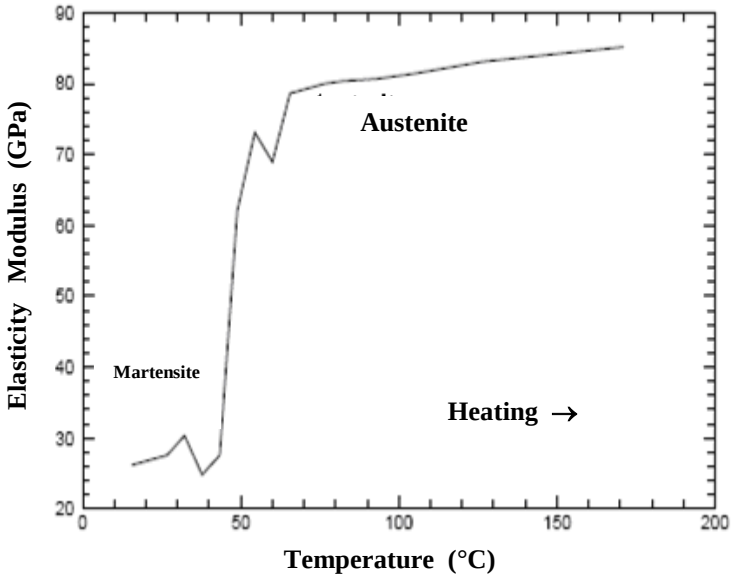

Figure 1. Elasticity Modulus of a Ni-Ti wire from T < Mf up to T > Af (Turner, 2000).

2. MATERIALS AND METHODS

2.1 Fabrication of the beams

Initially, due to its simplicity and low cost, hand layup process without vacuum bag, with consolidation inside closed moulds (i.e. male and female combined), was chosen for the fabrication of the SMAHC beams investigated in this work. The constituents adopted were: (i) cold cure (25°C) and hot cure (80 °C) epoxy resins from Maxepoxi; (ii) E-glass chopped fibers mat; and (iii) Ni(55.5%)–Ti(44.5%) wires from Memry GmbH, washed with the reagent Kroll (Faluhelyi, 2013). The basic geometry of the specimens, with length over thickness greater than 16, was based on the ASTM standard D 790-10. An external steel device to keep the Ni-Ti wires stretched during the consolidation of the epoxy matrix was attached to an internal aluminum female mould, as illustrated in Fig. 2.

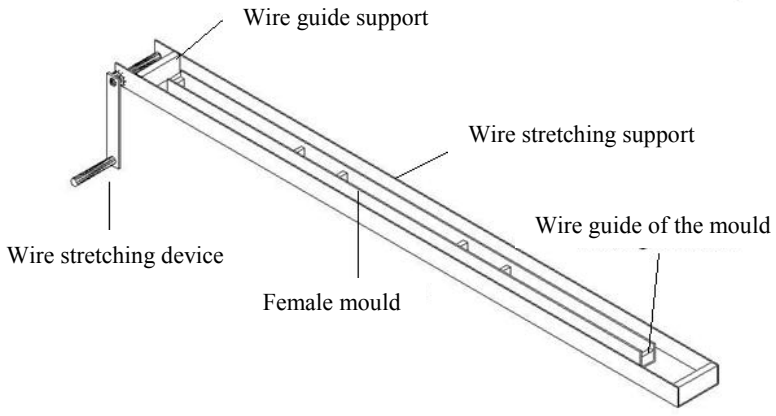

Figure 2. Stretching device and female mould.

The female mould presented in Fig. 2 is 1200 mm long and endowed with sets of aluminum blocks with uniformly distributed holes to guide the Ni-Ti wires. It is an U shape aluminum bar, with internal width of 31.3 mm, which is fixed on the steel base wire stretching support. In the fabrication of the beams, one extremity of the wires is fixed in a guiding block and the other end is griped and pulled by the lever of the stretching device. Thus, during the lamination of the E-glass/epoxy plies, the wires are kept straight until the resin is totally cured. As far as the cure temperature of the matrix is concerned, the specimens were divided into two main groups: cold (25°C) and hot (80°C) cure. For the cold cure group the epoxy system LY1316/HY1208 (glass transition temperature Tg = 60°C) was used to impregnate the E-

ISSN 2176-5480

glass mat and Araldite-F/HY956 (Tg = 80°C) to impregnate the wires; whereas for the hot cure group the system LY1316/HY1316 (Tg > 80°C) was adopted for all the layers. The cure cycle for the cold system is single stage, 24 hours at 25 °C (i.e. room temperature); and for the hot system two stages, with pre cure at room temperature for 10 hours, followed by a post cure at 80 °C for 7 hours. Initially, the layers of E-glass mat (450 g/m^2), as well as the wires, are cut and weighted in a digital scale and their total mass, m_f and m_w , respectively, are registered. When the specimens are extracted from the moulds their total weight, m_T, is measured. With these values it is possible to calculate the mass of matrix, m_m , and the respectively mass fractions of matrix, fibers and wires. In addition, with the densities of the constituents it is possible to obtain the respective volume fractions, V_f , V_w and V_m .

The SMAHC beams, with 19 plies, were fabricated in the aluminum U shape female mould, which was previously covered with a layer of release wax. The typical cross section of the beams, with the geometric details incorporated, is presented in Fig. 3. The symmetric lamination starts with two layers of E-glass mat/epoxy, followed by one layer Ni-Ti /epoxy and thirteen (13) E-glass/epoxy plies. And, since the stacking sequence is symmetric about the middle surface (i.e. at t/2), the last layers of Ni-Ti/epoxy (1) and E-glass/epoxy (2) have the same materials and thickness as the initial ones (i.e. the number of plies, in sequence, is: 2+*1*+13+*1*+2, where the symmetric Ni-Ti layers are represented in bold and italic). Fig. 3 refers to a beam with 8 Ni-Ti wires, 4 above the middle surface and 4 below. The nominal length of all the six beams manufactured in this work was C = 300 mm and the width b = 31.3 mm.

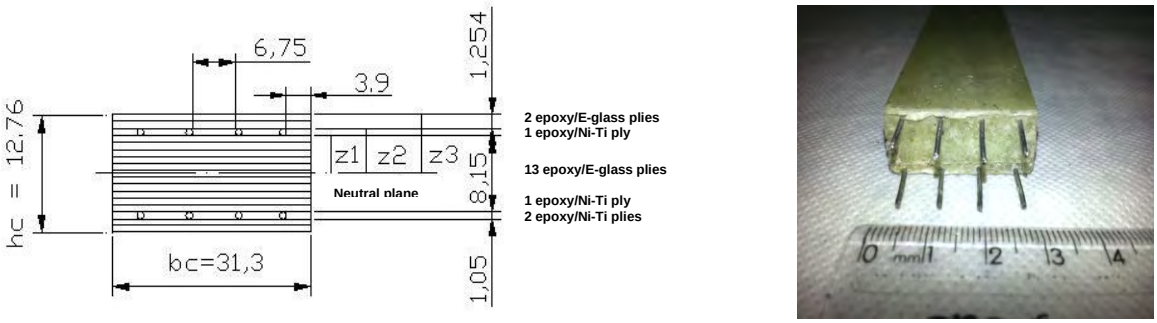

Figure 3. Cross-section views of the SMAHC beam with 19 plies (dimensions in mm).

The first six beams were fabricated without wires. The laminate of beams 01 to 03 consisted of 10 layers of E-glass/epoxy and, for beams 04 to 06, 21 plies of E-glass/epoxy, as presented in Tab. 1. Since the Ni-Ti SMA is very expensive, costing about US$ 1000/kg, in the next two specimens 8 wires of special galvanized alloy (SGA) were used, 4 above the mid-plane and 4 below, mainly to get experience in the manufacturing process which is rather complex and need, at least, two well trained operators. The nominal diameter of the SGA wires was 0.89 mm.

Table 1. Identification and main characteristics of the beams reinforced with E-glass, SGA and Ni-Ti.

Specimen	Characteristics	Average thickness (mm)	Standard Deviation (mm)	Total mass (grams)	V_f %	V_w %	V_m %
01	Without wires/no vacuum/cold cure	5.90	0.17	78	29.54	-----	64.65
02	Without wires/no vacuum/cold cure	5.90	0.17	78	29.54	-----	64.65
03	Without wires/no vacuum/cold cure	5.90	0.17	78	29.54	-----	64.65
04	Without wires/no vacuum/cold cure	10.54	0.21	160	36.06	-----	58.15
05	Without wires/no vacuum/cold cure	13.82	0.27	200	27.98	-----	66.21
06	Without wires/with vacuum/hot cure	7.52	0.17	121	45.54	-----	54.46
07	8 SGA wires/no vacuum/cold cure	11.64	0.24	169	26.22	1.72	68.51
08	8 SGA wires/no vacuum/cold cure	15.14	0.54	227	27.81	1.30	67.34
09	4 Ni-Ti wires/with vacuum/hot cure	8.93	0.22	131	38.36	1.23	60.41
10	6 Ni-Ti wires/with vacuum/hot cure	11.79	0.22	173	29.94	1.40	68.66
11	8 Ni-Ti wires/no vacuum/cold cure	12.29	0.37	180	22.54	1.76	72.50
12	8 Ni-Ti wires/no vacuum/cold cure	14.37	0.31	208	22.67	1.53	75.84
13	8 Ni-Ti wires/roving/vacuum cold cure	13.76	0.14	203	26.42	1.60	71.98
14	8 Ni-Ti wires/no vacuum/hot cure	12.55	0.22	182	25.35	1.74	65.37
15	8 Ni-Ti wires/roving/vacuum/hot cure	11.41	0.15	174	30.11	1.94	61.98
16	8 Ni-Ti wires/roving/vacuum/hot cure	12.40	0.13	178	28.83	1.78	63.32

ISSN 2176-5480

Finally, the last eight beams, incorporating two symmetric layers reinforced with up to four Ni-Ti wires of nominal diameter 1.05 mm, in each active ply, as presented in Fig. 3, were manufactured. The total thickness and mass of the beams, as well as the volume fractions of the constituents (i.e. V_f , V_w and V_m) are presented in Tab. 1. The beams 13, 15 and 16, were also reinforced with E-glass rovings between the Ni-Ti wires.

2.2 Characterization of the materials and specimens

Most of the physical and mechanical properties of the materials employed in this work (i.e. epoxy resin, E-glass fibers as well as special galvanized alloy (SGA) and Ni-Ti wires) were obtained from the literature (Daniel and Ishai, 2006; Levy-Neto and Pardini, 2006; Janocha, 1999; Srinivasan and McFarland, 2001) and from the catalogs of the manufacturers of the products. The mass and average diameter of 1 m long Ni-Ti wires were measured, in order to calculate the density of the adopted SMA. In addition, the elasticity modulus (E) and tensile strength of 150 mm long Ni-Ti wires, with glass/epoxy tabs, in the martensitic (E_M) and austenitic (E_A) phases, tested in a MTS-810 machine, at 25 °C and 69 °C, respectively, were obtained experimentally. The density, elasticity modulus and tensile strength of the materials used are presented in Tab. 2. The elastic behavior and the natural frequencies of the produced beams were obtained experimentally, analytically and numerically (using the finite element program ANSYS),

Table 2. Physical and mechanical properties of the materials.

Material	Density (g/cm^3)	Elasticity Modulus (GPa)	Tensile Strength (MPa)
Special galvanized alloy (SMA) wires	6.63	75	240
E-glass fibers	2.54	70	2400
Epoxy resin (LY1316/HY1208)	1.05	3.5	55
Ni-Ti wires/Martensitic phase	6.45	22.6	700
Ni-Ti/Austenitic phase	6.45	48.4	1500

2.3 Temperature control system

In order to increase the temperature of the wires to 69 °C, based on the Joule effect, a controlled electric current was applied on them, using schematic setup presented in Fig. 4. A closed loop electronic circuit that measures the temperature and controls the current was developed for this purpose. Since the specimens and test machine are metallic and conduct electricity, the jaws that hold the wires were carefully insulated. The Ni-Ti wires were assembled in series and connected to a 12 volts D.C. power unit. Details about the on-off control system can be found in Céron (2010). The heating system represented in Fig. 4 was used to control the temperature of single Ni-Ti wires as well as SMAHC beams. In the hybrid beams, the embedded Ni-Ti wires were connected in series. Thus the same electric current flows throughout all the Ni-Ti wires.

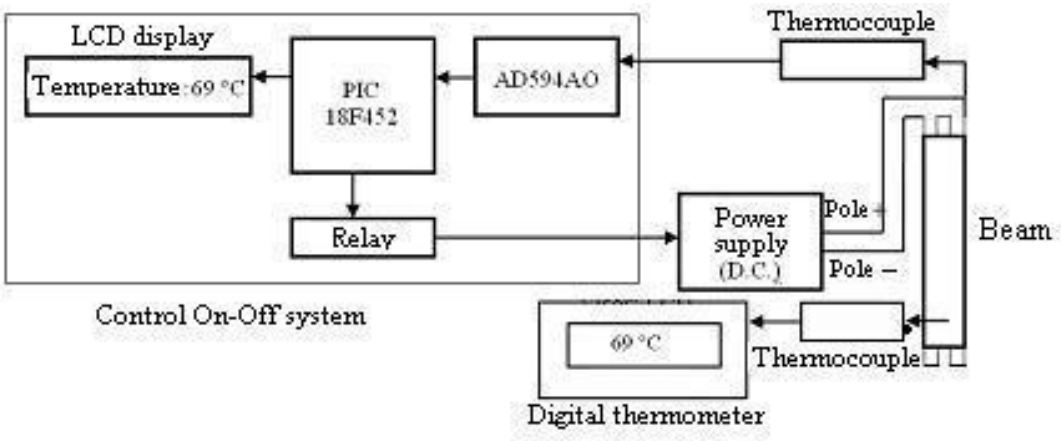

Figure 4. Schematic view of the temperature control system

ISSN 2176-5480

3. MATEMATICAL MODEL OF THE HYBRID BEAMS

3.1 Static analysis of the beams

In order to analyze the static bending stiffness of the composite beam with functional SMA wires as well, as structural E-glass fibers embedded in an epoxy matrix material, it is necessary to account for the effect of the Ni-Ti on the elastic properties of the SMAHC and for its main role to increase the effective flexural modulus (E_F), during the phase transformation from martensite (E_M) to austenite ($E_A \cong 2.E_M$, obtained experimentally in this work). Due to the fact that epoxy resin is an excellent adhesive and the Ni-Ti wires are strait and parallel to the longitudinal direction it is natural to treat them as unidirectional reinforcement in the matrix of the composite material, whose constituent properties are known. This allows the use of classical lamina and laminate macromechanical equations (Gibson, 1994; Levy Neto and Pardini, 2006) to estimate the influence of Ni-Ti wires volume fraction and placement, along z direction, on the flexural modulus (E_F), in particular Eq.(1), for symmetric laminated beams. The representation of such beams is shown in Figs. 3 and 5, where x is the longitudinal axis and z the vertical distance from the middle surface of the beam. Using Eq. (1), in order to obtain the effective flexural modulus of the hybrid beam (E_F), deflections of SMAHC beams (δ) can be calculated by using E_F in place of the elasticity modulus (E) in the beam deflection equation for three point bending loading (2), in the elastic regime, from elementary mechanics of materials (Gibson, 1994).

$$E_F = \frac{8}{t^3} \cdot \sum_{j=1}^{N/2} (E_x)_j \cdot (z^3{}_j - z^3{}_{j-1}) \tag{1}$$

where: t is the total thickness of the beam; N is the total number of plies; j is the index of each ply and varies from 1 to N ($1 \le j \le N$); $(E_x)_j$ is the elasticity modulus of each ply in the longitudinal direction x of the beam; and z is the vertical distance measured from the middle surface of the symmetric beam (i.e. at t/2). It is important to notice that the contribution of each layer in E_F depends on the third power of the distance of the ply, measured from the middle plane, i.e. z^3.

$$\delta = (P \,.\, L^3) \,.\, (48.\, E_F \,.\, I)^{-1} \tag{2}$$

where: P is the applied load at mid span, L is the span and $I = (b.t^3)/12$ is the cross section moment of inertia, measured from the middle surface; t is the total thickness obtained from Tab. (1) and b=31.3 mm is the width of the beams.

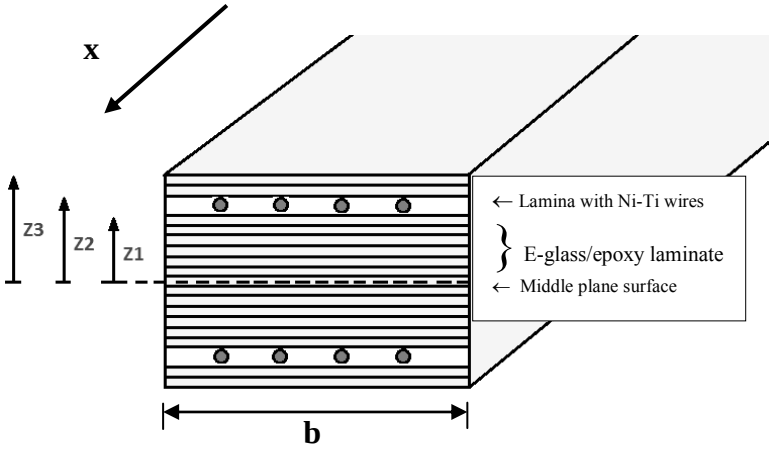

Figure 5. Schematic representation of a symmetric laminated SMAHC beam.

The elasticity modulus of the composite layers $(E_x)_j$ were calculated using Eq. (3) obtained from Mendonça (2005), for the plies of E-glass chopped mat/epoxy (E_{GE}); and from the rule of the mixtures, Eq. (3), given by Daniel and Ishai (2006), combined with Eq. (2), for the layers reinforced with Ni-Ti wires (E_{SMA}).

$$E_{GE} = 3.44 + 28.2\, V_f + 21.6\, V_f^4 \tag{3}$$

where: V_f is the volume fraction of chopped E-glass fibers in the E-glass/epoxy plies.

For the layers of Ni-Ti/epoxy in particular the SMA wires can be modeled as unidirectional reinforcement and the resulting longitudinal elasticity modulus ($E_{SMA/E}$) can be calculated using Eq. (4), based on the micromechanics approach (Gibson, 1994), since the Ni-Ti wires (E_{SMA}) the matrix (E_m) and, only in the case of the active plies reinforced with E-glass rovings (E_{rov}), are subjected to the same longitudinal strain.

ISSN 2176-5480

$$E_{SMA/E} = E_{SMA} \,.\, V_{SMA} + E_m \,.\, V_m \; + E_{rov} \,.\, V_{rov} \tag{4}$$

where: V_{SMA} and V_m are the volume fractions of wires (SMA) and matrix (m) in these particular plies.

3.3 Dynamical behavior of the beams

In order to evaluate the potential of the heated Ni-Ti wires to change the natural frequencies of the SMAHC beams, the specimens were also subjected to impulsive forces, with free-free boundary condition, as shown schematically in Fig. 6. All beams were previously tested showing damping factor below 0.06, so the damping effects in natural frequencies of the beams were neglected (Thomson, 1978). In such situation, and assuming an Euler-Bernoulli model for symmetric beams, constituted of homogeneous or orthotropic material plies, Eq. (5) presents their natural frequency (Carpenter, 1977; Thomson, 1978; Ewins, 1984; Faluhelyi, 2013). Figure 6 shows more details of the vibration tests, in which the beams were suspended, at both extremities, by elastic strips inside an steel frame and exited by an instrumented hammer. The experimental frequencies of all beams, up to 3rd mode, were determined using Eq. (5), considering that the plane of vibrations is represented by X-Z, where X and Z axis are along the length and the thickness of the beams, respectively. Using the element Beam 189 of ANSYS, the natural frequencies of the beams were also obtained numerically.

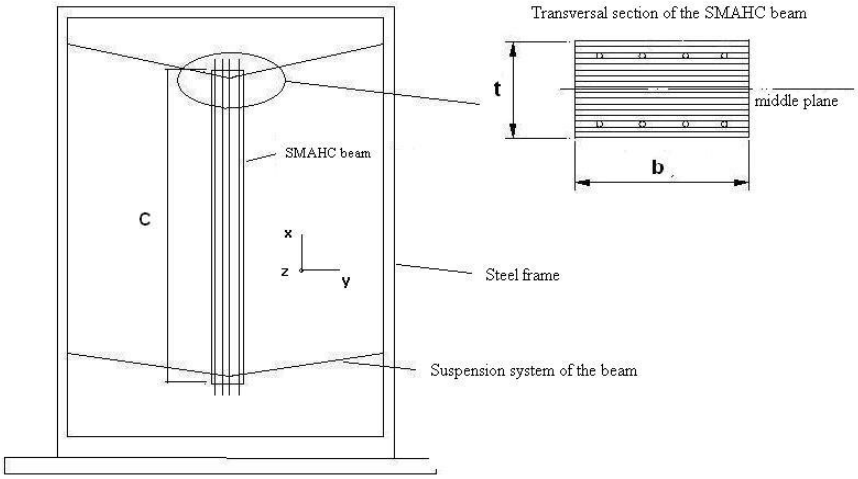

Figure 6. Diagram of SMAHC beam suspended at the ends by elastic trips on a steel frame.

$$f_n = \frac{(gC)_n^2}{4\pi} \frac{t}{C^2} \sqrt{\frac{E}{3\rho}} \quad , \tag{5}$$

where $(gC)_n^2$ is the boundary condition factor, for n modes; t is the thickness, C is the length, E elasticity modulus and ρ density. The factors $(gC)_n^2$, for n=1, 2 and 3, respectively, are 22.4, 61.7 and 121 (Thomson, 1978).

4. EXPERIMENTAL AND THEORETICAL RESULTS

The beams were tested in three points bending, following ASTM Standard D 790-10, under static loads in the elastic regime at 25 °C and 69 °C. Figure 7 shows a typical SMAHC beam, subjected to bending loads, at $T>A_f$, in the universal machine MTS 810.The vertical loads (P), at a rate of 1 mm per minute, were applied at the midspan (L/2), using the MTS 810 machine. In all the tests the span (distance between the supports at the extremities) was L = 280 mm and the maximum deflection (δ) was given by Eq. (2). The maximum deflection was kept below L/100 in all tests. Thus, from the values of P and δ, obtained from the MTS machine, as well as the span L = 280mm, and I, it was possible to obtain E_F experimentally. In addition, using Eq. (1), was possible to calculate E_F theoretically. These results are presented in Table 3. For the beams 9 to 16 the tests were carried out with the Ni-Ti wires at 25 °C (martensite phase, M) and 69 °C (austenite phase, A). At 25 ^oC the elasticity modulus of the SMA wires is E_M = 22.6 GPa, whereas for 69 ^0C the modulus increases to E_A = 48.4 GPa.

ISSN 2176-5480

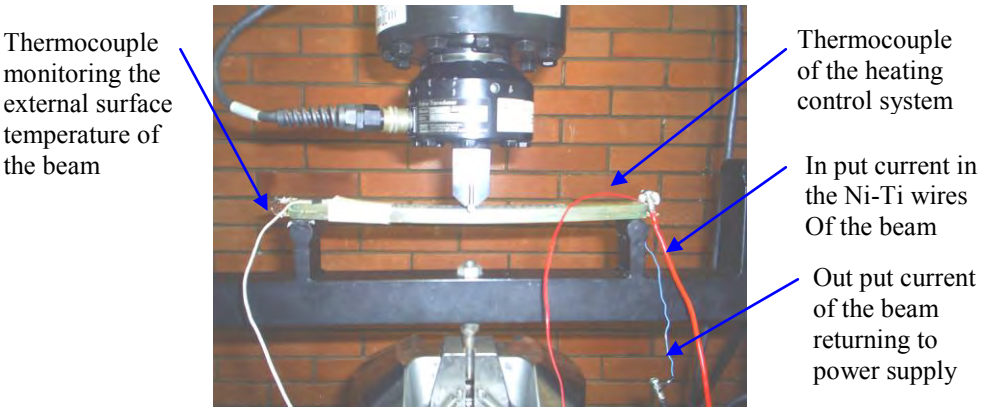

Figure 7. Three point bending static flexural test in a SMAHC beam at 69 ºC > A_f.

Table 3. Experimental and theoretical results for the bending elastic modulus of the SMAHC beams.

Specimen[1]	Flexural modulus (GPa)		Percentage differences[2] (%)
	Analytical (E_{theo})	Experimental (E_{exp})	
01	11.94	10.50	+ 13.61
02	11.94	11.71	+ 1.96
03	11.94	11.90	+ 0.34
04	13.97	13.81	+ 0.34
05	11.46	11.41	+ 1.16
06	17.21	17.17	+ 0.23
07	10.53	10.52	+ 0.10
08	11.16	10.90	+ 2.39
09M	16.15	13.79	+ 17.11
09A	16.62	14.02	+ 18.54
10M	14.01	13.98	+ 14.09
10A	14.57	13.30	+ 20.02
11M	9.53	9.50	+ 0.32
11A	10.25	10.12	+ 1.28
12M	10.02	9.77	+ 2.56
12A	10.83	9.91	+ 9.28
13M	13.44	12.34	+ 8.91
13A	14.09	14.36	- 1.89
14M	10.59	8.60	+ 23.14
14A	11.57	9.38	+ 23.35
15M	14.25	12.84	+ 10.98
15A	15.02	12.88	+ 16.61
16M	13.80	11.64	+18,56
16A	14.52	11.66	+24.53

[1] tested at 25 ºC and 69 ºC, in the martensític (M) and austenitic (A) phase of Ni-Ti wires, respectively.
[2] percentage values calculated using the expression: $(E_{Theo} - E_{Exp} / E_{Exp}) \times 100$.

Figure 8 shows a typical SMAHC beam, with eight Ni-Ti wires (four in which active ply, symmetric from the middle surface), ready to be instrumented and tested in the MTS-810 universal machine. For the tests at 69 ^{0}C, with the wires in the austenitic phase, the 8 Ni-Ti wires are electrically connected in series and subjected to a controlled electrical current, in order to heat them up. Before the vertical load P is applied, the temperature of the wires is stabilized at 69 ^{0}C, by means of the temperature control system, shown schematically in Fig. 4, and this temperature is maintained until the end of the mechanical bending test. Figure 9 presents the diagram force (P) versus deflection (δ) of the SMAHC beam 13. Table 4 presents variations in the SMAHC beams elastic modulus, when the wires are heated.

ISSN 2176-5480

Figure 8. SMAHC beam ready to be instrumented for the bending test

Figure 9 shows diagrams of force (P) versus mid span deflection (δ) of the beam 13, at 25 ºC (martensite, Fig. 9.a) and 69 ºC (austenite, Fig. 9.b). The double arrows at the plots are related to uncertainties in P and δ measurements.

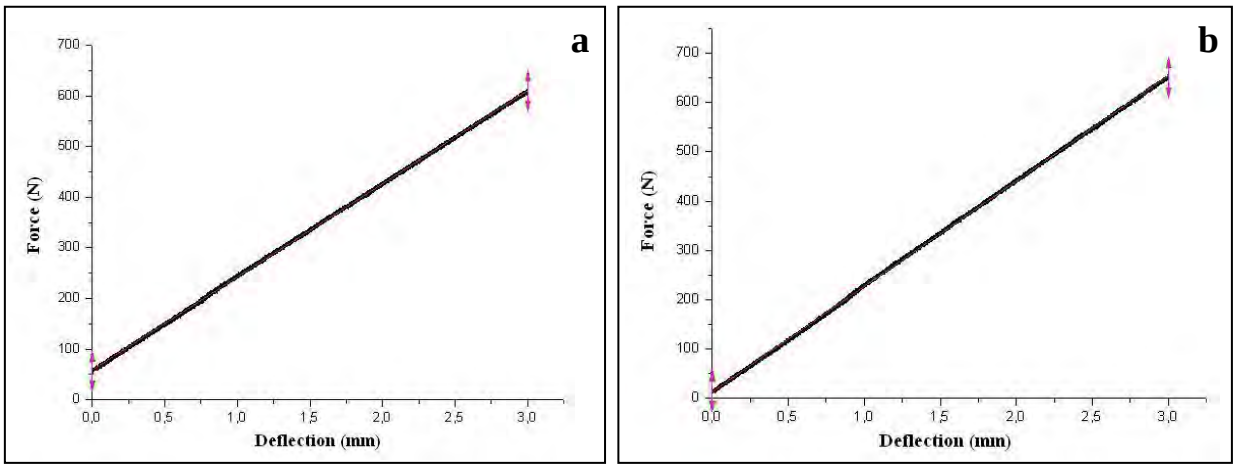

Figure 9. Diagrams Force (P) versus Deflection (δ), beam 13 at (a) martensite (25^0C) and (b) austenite phase (69^0C)

Table 4. Experimental and theoretical changes in the beams flexural modulus when the Ni-Ti wires are heated

Specimen[(1)]	Flexural modulus (GPa)		Percentage increase (%)
	in martensite phase	in austenite phase	
9AN	16.15	16.62	+ 2.91
9EXP	13.79	14.02	+ 1.69
10AN	14.01	14.57	+ 4.00
10EXP	13.98	13.30	- 4.86
11AN	9.53	10.25	+ 7.56
11EXP	9.50	10.12	+ 6.53
12AN	10.02	10.83	+ 8.08
12EXP	9.77	9.91	+ 1.43
13AN	13.44	14.09	+ 4.84
13EXP	12.34	14.36	+ 16.37
14AN	10.59	11.57	+ 9.25
14EXP	8.60	9.38	+ 9.07
15AN	14.25	15.02	+ 5.40
15EXP	12.84	12.88	+ 0.31
16AN	13.80	14.52	+ 5.22
16EXP	11.64	11.66	+ 0.17

ISSN 2176-5480

Table 4 shows the analytical (AN) and experimental (EXP) variation in the bending elasticity modulus of the SMAHC beams, when the Ni-Ti wires are heated from 25 ^{0}C to 69 ^{0}C and the phase transformation from martensite to austenite takes place. Table 5 presents relative differences between numerical and analytical natural frequencies of the beams, up to 3rd mode, respectively. The numerical results were obtained using the element Beam 189, with 200 nodes, from ANSYS, adopting free-free boundary conditions. The analytical results were obtained from Eq. (5).

Table 5. Analytical and numerical (ANSYS) natural frequencies of the beams in first three modes

Specimen	Natural frequencies (Hz)						Percentage differences* (%)		
	Numerical (f_{nu})			Analytical (f_{an})					
	1st	2nd	3rd	1st	2nd	3rd	1st	2nd	3rd
01	189.16	520.06	1025.30	177.93	490.11	961.16	+ 6.31	+ 6.11	+ 6.67
02	189.16	520.06	1025.30	187.82	517.33	1014.54	+ 0.72	+ 0.53	+ 1.06
03	189.16	520.06	1025.30	189.33	521.51	1022.74	- 0.09	- 0.28	+ 0.25
04	329.57	901.63	1748.40	354.99	977.82	1917.60	- 7.16	- 7.79	- 8.82
05	424.79	1157.20	2231.40	414.50	1090.00	2231.00	+ 2.48	+ 6.17	+ 0.02
06	271.73	746.34	1455.50	272.72	751.20	1473.19	- 0.36	- 0.65	- 1.20
07	328.63	897.35	1735.50	348.91	961.05	1884.71	- 5.81	- 6.63	- 7.92
08	450.06	1223.30	2351.80	455.88	1255.70	2462.55	- 1.28	- 2.58	- 4.50
09M	327.18	897.33	1746.40	304.01	837.37	1642.17	+ 7.62	+ 7.16	+ 6.35
09A	331.91	910.29	1771.60	306.53	844.32	1655.80	+ 8.28	+ 7.81	+ 6.99
10M	401.48	1097.00	2124.20	403.98	1112.74	2182.20	- 0.62	- 1.41	- 2.66
10A	409.42	1118.80	2166.20	394.03	1085.34	2128.47	+ 3.91	+ 3.08	+ 1.77
11M	336.18	916.83	1770.20	350.53	965.53	1893.51	- 4.09	- 5.04	- 6.51
11A	348.85	952.86	1844.00	361.79	996.54	1954.32	- 3.58	- 4.38	- 5.64
12M	415.59	1131.00	2177.80	414.42	1141.51	2238.62	+ 0.28	- 0.92	- 2.72
12A	432.06	1175.80	2264.10	417.38	1149.66	2254.60	+ 3.52	+ 2.27	+ 0.42
13M	456.65	1241.60	2387.10	429.16	1182.11	2318.24	+ 6.41	+ 5.03	+ 2.97
13A	480.98	1307.70	2514.30	437.55	1205.22	2363.56	+ 9.93	+ 8.50	+ 6.38
14M	367.38	1002.90	1939.50	341.33	940.18	1843.79	+ 7.63	+ 6.67	+ 5.19
14A	384.00	1048.30	2027.30	356.45	981.84	1925.49	+ 7.73	+ 6.77	+ 5.29
15M	385.89	1053.50	2037.00	366.98	1010.84	1982.35	+ 5.15	+ 4.22	+ 2.76
15A	396.18	1081.60	2091.30	367.55	1012.41	1985.44	+ 7.79	+ 6.83	+ 5.33
16M	416.42	1135.00	2189.50	392.38	1080.81	2119.57	+ 6.13	+ 5.01	+ 3.30
16A	427.14	1164.20	2245.90	392.72	1081.74	2121.39	+ 8.76	+ 7.62	+ 5.87

Table 6. Numerical (NU) and analytical (AN) natural frequencies variations by changing phase of Ni-Ti wires.

Specimen[(1)]	Natural frequencies (Hz)		Percentage variation[(2)] (%)
	martensite (f_M) 25 ^{0}C	in austenite (f_A) 69 ^{0}C	
09NU	327.18	331.91	+ 1.45
09AN	304.01	306.53	+ 0.83
10NU	401.48	409.42	+ 1.98
10AN	403.98	394.03	- 2.46
11NU	336.18	348.85	+ 3.77
11AN	350.53	361.79	+ 3.21
12NU	415.59	432.06	+ 3.96
12AN	414.42	417.38	+ 0.71
13NU	456.65	480.98	+ 5.22
13 AN	429.16	437.55	+ 1.96
14NU	367.38	384.00	+ 4.52
14AN	341.33	356.45	+ 4.43
15NU	385.89	396.18	+ 2.67
15AN	366.98	367.55	+ 0.16
16NU	416.42	427.14	+ 2.57
16AN	392.38	392.72	+ 0.09

[(1)] Numerical (NU) and analytical (AN) results in martensite (25 ºC) and austenite (69 ºC).
[(2)] Percentage values were calculated using the expression: $(f_A - f_M)\,x100/\,f_M$.

ISSN 2176-5480

Table 6 shows the percentage variations in numerical (NU) and analytical (AN) natural frequencies of SMAHC beams, due to the phase transformation, from martensite to austenite (at 69 ^{0}C), of the Ni-Ti wires, for the 1st vibration mode. In 15 out of 16 predictions, the numerical and analytical calculations obtained higher natural frequencies, by factors up to 5.22% and up to 4.43%, respectively, after the temperature was increased to 69 ^{0}C.

5. ANALYSIS AND DISCUSSION OF RESULTS

5.1. General aspects of the fabrication of SMAHC beams

The fabrication method incorporating a stretching device, developed in this study, worked satisfactorily at both cure temperatures, 25°C and 80°C, mainly for the Ni-Ti wires, due to the fact that it was easier to keep the ticker Ni-Ti wires (diameter 1.05 mm) stretched and well fixed at the extremities during the manufacturing process. SMAHC beams, with volume fraction of E-glass chopped fibers, V_f, in the range from 22.54% to 45.54% were obtained. This variation in fiber content took place due to the fact that only few specimens were consolidated inside a vacuum bag. For most of the specimens, instead of a vacuum bag, an external pressure of about 0.2 bar (0.02 MPa) was applied on the top surface of the male mould (which moves), by means of leaving heavy metal pieces on it during the consolidation of the composites. For the beams consolidated without vacuum, part of the prepared resin (i.e. the excess) came out from the mould and made the extraction of the specimens rather difficult. However, for the SMAHC beams produced without vacuum, the volume fraction of epoxy resin was higher; the stiffness of the E-glass/epoxy was lower, and the relative increase in bending stiffness due to the phase transformation of the Ni-Ti wires was higher. When the Ni-Ti wires are heated, their elasticity modulus increase from 22.6 to 48.4 GPa. Thus, since the elasticity modulus of E-glass fibers is 70 GPa, and the one for epoxy resin 3.5 GPa, the lowest is the volume fractions of E-glass, the higher will be influence of the Ni-Ti wires on the bending stiffness of the SMAHC beams.

5.2. Elastic behavior of SMAHC beams in bending tests

As shown in Table 3, for 93.75% of the beams (there was only one exception in 16 specimens), the theoretical (i.e. analytical) values of the flexural modulus of the beams were always higher than the experimental, by factors varying from -1.89 % to 24.53 %. This suggests that the theoretical model, in which all interfaces (i.e. epoxy/E-glass and epoxy/wires) are assumed to be perfect, overestimates the bending stiffness, of the specimens fabricated and tested in this work.

Considering the 8 SMAHC beams (specimens 9 to 16), with active Ni-Ti wires incorporated, it was noticed that for 87.5% of the tests at 69 ºC (7 out of 8 tests), both the theoretical as well as the experimental flexural modulus were higher than those of 25 ºC. Only for the experimental result of beam 10 (with only 6 Ni-Ti wires), the elasticity modulus decreased (4.86%) when the Ni-Ti wires were heated. This confirms that all the SMAHC beams with 8 Ni-Ti wires (specimens 11 to 16), in the austenitic phase, are stiffer in bending, up to 16.37%. The increases in stiffness are moderate, as shown in Table 4, but the volume fraction of wires in these specimens was in the range of only 1.23 to 1.94 %. The Ni-Ti wires are very expensive and difficult to incorporate in the composite beams. So, the strategy adopted in this investigation was to work only with up to 8 wires, in two layers of 4, but keeping such layers as far as possible from the middle surface of the SMAHC beams. The reason for this is the fact that, according to Eq. (1), in a laminated beam, the contribution of a generic ply (i) is proportional to $(z_i^3 - z_{i-1}^3)$, where z_i and z_{i-1} (see Figs. 3 and 5) are the distances from the middle plane, where a layer ends and begins, respectively (Gibson, 1994; Levy-Neto and Pardini, 2006). Thus, since z_i and z_{i-1} are in the third power, this non linear geometric effect amplifies the contribution of the plies which are located far from the middle plan and allows one to reduce costs and use, as effectively as possible, minimum amounts of Ni-Ti in a SMAHC beam.

For SMAHC specimen 11, with the Ni-Ti wires at 69 ºC, the theoretical and experimental flexural moduli were higher than those for 25 ºC, by 7.56% and 6.53%, respectively. And, for specimen 14, the theoretical and experimental moduli increased 9.25% and 9.07%, respectively, for the same variation in temperature (increase of 44 ^{0}C). For these specimens (11 and 14, both with 8 Ni-Ti wires), the theoretical and experimental variations in the elasticity modulus were consistently close to each other. For all the 8 SMAHC beams, the theoretical prediction was always an increase in the bending modulus, when the temperature is elevated in 44 ^{0}C. This analytical estimation is not a surprise since, as the temperature rises from 25 ^{0}C to 69 ^{0}C, the elastic modulus of the Ni-Ti wires increases from 22.6 GPa to 48.4 GPa. And, in 7 out of 8 cases, the increase in the elasticity modulus of the SMAHC beams was confirmed experimentally. The only exception was for beam 10 (with only 6 Ni-Ti wires) in which, experimentally, the elasticity modulus decreased 4.86%, whereas the analytical prediction was to increase 4%. Thus, in 87.5% of the tests, the experimental results confirmed that the bending stiffness of the SMAHC increases, when the temperature of the Ni-Ti increases 44 ^{0}C, indicating that the SMAHC incorporating 8 Ni-Ti wires, produced in this investigation, can work as an adaptative structure. The variations in the natural frequencies of the beams due to the same increase in the temperature, presented in tables 5 and 6, confirm the observed variations in stiffness.

ISSN 2176-5480

6. CONCLUSIONS

All the 6 SMAHC beams, which incorporated 8 Ni-Ti wires, presented higher experimental bending modulus (in the range 0.17% to 16.37%), when heated from 25 ^{0}C to 69 ^{0}C.

Another important conclusion regarding the SMAHC beams fabricated in this study, as reported in Table 4, is the fact that both, theoretical and experimental, flexural modulus increased up to 9.25% and 16.34%, respectively, when the temperature of the wires increased from 25 ºC to 69 ºC. The maximum volume fraction of wires was 1.94% and an increment of 44 ºC in temperature increased the experimental flexural modulus for 87.5% of the specimens (7 out of 8 beams), indicating that the bending stiffness, as predicted theoretically, can be controlled by means of the phase transformation of the Ni-Ti wires, from martensite to austenite, induced by the electric current.

The fabrication process adopted, without vacuum bag, was satisfactory, mainly for the manufacturing of the SMAHC beams, which presented repeatable characteristics such as thickness, mass as well as volume fractions of matrix, E-glass and Ni-Ti wires. In addition, since for the beams with less volume fraction of E-glass fibers the increase in stiffness, due to the temperature elevation of the Ni-Ti, is highlighted (the initial stiffness is lower), the SMAHC beams consolidated without vacuum woks better as an adaptative structure than those consolidated in a vacuum bag.

7. ACKNOWLEDGEMENTS

The authors are grateful for the support they received from PETROBRAS and ELETRONORTE.

8. REFERENCES

Carpenter, S. T., 1977, “Structural Mechanics”. John Wiley, New York, 479 p.

Cerón, D.M.S., 2010, “Development of a methodology for the fabrication of Shape Memory Alloy Hybrid Composites”. Dissertação de Mestrado em Ciências Mecânicas, Departamento de Engenharia Mecânica, Universidade de Brasília, 100p. (in Portuguese)

Daniel, I.M. and Ishai, O., 2006, "Engineering Mechanics of Composite Materials", Oxford University Press, Second Edition, Oxford, 411 p.

Ewins, D. J., 1984, “Modal Testing: Theory and Practice. John Wiley, 347 p.

Faluhelyi, P., 2013, “Fabrication and Thermomechanical Behavior of Adaptative Structural Composite with Ni-Ti Filaments”. Tese de Doutorado, Department of Mechanical Engineering, University of Brasília, 225 p. (in Portuguese)

Ghandi, M.V. and Thomson, B.S., 1992, “Smart Materials and Structures”. Chapman e Hall, London, 309 p.

Gibson, R.F., 1994, “Principles of Composite Material Mechanics”. McGraw-Hill Inc., New York. 425 p.

Janocha, H. (Editor), 1999, “Adaptronics and smart structures – Basics, materials, design and applications”. Springer – Verlag, Berlin, 438 p.

Levy-Neto, F. and Pardini, L.C., 2006, “Structural Composites, Science and Technology”. First Edition, Edgard Blücher, São Paulo, 313p. (in Portuguese)

Mendonça, P. T. R., 2005, “Composites Materials and Sandwich Structures”. Ed. Manole, 656p. (in Portuguese)

Otsuka K. and Wayman C. M., 1998, “Shape Memory Materials. Cambridge”. University Press.

Perkins, J., 1981, “Shape Memory Behavior and Thermoelastic Martensitic Transformations”. Materials Science and Engineering, 51, p. 181-192.

Rogers, C.A. and Robertshaw, H.H., 1988, ”Shape Memory Reinforced Composites”. Engineering Science Preprints 23, ESP2588027, Society of Engineering Sciences.

Rogers, C. A. and Robertshaw, H. H., 1993, “Intelligent Material Systems–The Dawn of a New Materials Age”. Journal of Intelligent Materials System and Structures, Vol. 4, Technomic Publishing Company, Lancaster, U.S.A..

ScienceDirect. http://www.sciencedirect.com. Acessed in 20/04/2010.

Srinivasan, A.V. and McFarland, M. D., 2001, “Smart Structures Analysis and Design”. Cambridge University Press, Cambridge.

Turner, T.L., 2000, “Thermomechanical Response of Shape Memory Alloy Hybrid Composites”. NASA/TM-2001-210656, Langley Research Center, Hampton, Virginia, 2000.

Wayman, C. M., Duerig, T. W., 1990, Engineering Aspects of Shape Memory Alloys. Eds.: Duerig, T.W., Melton, K. N.,Stockel, D., Wayman, C. M. Butterworth-Heinemann. p. 3-20.

9. RESPONSIBILITY NOTICE

The authors are the only responsible for the printed material included in this paper.